Journal of Scientific & Industrial Research
Vol. 81, October 2022, pp. 1037-1049
DOI: 10.56042/jsir.v81i10.62442

Experimental and Numerical Investigation for Estimating Optimal Depth-Bearing Capacity of Randomly Fiber-Reinforced Sandy Soils

Şeyda DOĞAN KÜÇÜKÇONGAR[1], Semet ÇELIK[1]* & Babak KARIMI GHALEHJOUGH[2]

[1]Ataturk University, Civil Engineering Department, Erzurum, Turkey
[2]Erzurum Technical University, Civil Engineering Department, Erzurum, Turkey

Received 19 April 2022; revised 24 September 2022; accepted 26 September 2022

Reinforcing will lead to improved mechanical properties of soil. Using different additives can help to increase bearing capacity, strength, or other important properties. In this study, poorly graded sandy soil was improved by adding synthetic fiber, and a strip footing was placed and loaded on unreinforced and reinforced soil. Samples were prepared in two relative densities of 50% and 65% and the soil was reinforced in 1B, 2B, 2.5B, and 3B depths (B is width of model footing). Bearing capacity and shear failure surfaces of soil that were analyzed by the Particle Image Velocimetry (PIV) method at different settlement to footing width ratios were obtained and compared. At the same time, experimental conditions were modeled with finite element method, and the results of shear failure surfaces were compared with experimental modeling. Results showed that reinforcing the soil under the strip footing forwarded shear failure surfaces toward downer surfaces from 1B up to 3B. In soils with a relative density of 50%, the main reinforcing depth was 2B and after 2B reinforcing did not have a considerable effect on improving the soil. By increasing the relative density from 50% to 65%, the effective reinforcing depth increased from 2B to 2.5B. Experimental and numerical modeling of soil under strip footing showed that the optimum reinforcing depth was between 2B and 2.5B that by increasing the reinforcing depth, the general shear failure behavior went toward local shear failure surfaces. The results of the study can be used as a reinforcing method and applied to real soil improvement applications in industry depending on the purpose of soil reinforcing for economic and efficient improvement design.

Keywords: Finite element modeling, Particle image velocimetry, PIV, PLAXIS, Soil reinforcing

Introduction

In recent years' different methods have been used for improving the mechanical and chemical properties of different materials used in civil engineering applications. These methods can involve adding some chemical additives, geopolymers, fly ash, or lime that affect the physico-chemical properties or binder bonds.[1–3] Another method that can be used for improving the properties is using other materials without effecting the chemistry of the material. Using fibers is a method that has recently been offered as a discrete structure for the construction of fiber-reinforced soil structures. The discrete structure can be used to predict the comparable shear strength of soil reinforced with fiber based on independent characterization of soil and fiber properties. Initially, plant roots were used as reinforcement in geotechnical projects for fiber reinforcement. Wu *et al.* (1988) discovered that plant roots will lead to an increase in shear strength of soil that will make the natural slopes more atable.[4] Since the 1980s, when the first polymeric fiber research were undertaken, synthetic fibers have been used and effect of fiber reinforcement was investigated by doing unconfined compression, direct shear strength, and triaxial compression tests. Prior studies have demonstrated that reinforcement with fiber can significantly improve reinforced soil's peak shear strength while preventing loos of post-peak shear strength. Most of the experiments were carried out on granular soils. Gray & Ohashi (1983) used direct shear tests to investigate the mechanisms of fiber reinforcement.[5] Al-Refeai (1990) investigated on reinforcement effect using various aggregates that reinforced with fibers. Results showed that fiber reinforcement of granular soil was more effective in sub-rounded fine sand than in sub-angular medium-grained sand.[6]

There appear to be fewer studies on the application of reinforcement with fiber in cohesive soil samples. Although reinforcement with fiber has been proven to strengthen the shear strength of cohesive soils, more research is needed and necessary for better understanding of mechanisms of load transfer at the fiber-clay interface.

*Author for Correspondence
E-mail: scelik@atauni.edu.tr

Fiber-reinforcement design has historically been done by use of "composite" technique, that composite of fiber-soil is evaluated as a composite, an "equivalent" shear strength has been frequently used to determine the behavior of the material in shearing condition.[5] Fiber self-weight may result in preferable fiber orientation during mixing procedures. Within geotechnical engineering, traditional soil reinforcing methods need the application of continuous planar reinforcement inclusions like metallic strips, geotexiles and geogrids. Only one direction of soil tensile resistance is provided by the components. Since the shear strength of interface is generally lower than the soil, lines of instability and weakness can be generated along the interface between reinforcement and soil. Fiber-reinforcement techniques are increasingly being used in geotechnical applications such as failed slopes repairing and thin soil veneers stabilization. While many studies have been performed on the modeling and construction of buildings with continuous planar reinforcement, further research is needed for better understanding of behavior of randomly distributed fibers reinforced soils. According to a previous study, adding fibers to soil increases maximum shear strength while minimizing loose of strength in post-peak area. The change in strength properties caused by reinforcement is often studied by an increase in friction angle and cohesion, which is generally evaluated by testing fiber-reinforced composites. In today's geotechnical industry, designing a fiber-reinforcement project includes analysis of project-specific fiber-reinforced models, that can be costly and may need more time. A discrete approach based on independent characterisation of soil and fiber properties has recently been developed to prevent the needs for project-specific testing, even for small projects.[7] Reinforcing soil with fiber can affect different composite properties, like shear strength, stress-strain behavior; influence of fibers on soil compaction; hydraulic conductivity of fiber-reinforced soil. Reinforcement with fibers has also can be applied for stabilization of slopes, subbase or thin veneers and construction of embankments. The following are the general benefits of fiber reinforcement:

- Fibers can be placed in the field using typical construction equipment.
- Weather does not have a significant effect on fiber reinforcement.
- Materials suitable for reinforcement with fiber are widely available. In addition to synthetic fibers made in a factory, recycled fibers, shredded tires and plant roots can be used as reinforcing materials.[8,9]

Another application is the stability of landfill covers. Although continuous horizontal reinforcing is already used, it must be anchored into competent material beneath the soil veneer. In addition, parallel reinforcement to the slope necessitates the anchoring of the reinforcement at the top of the slope. Discrete fibers, on the other hand, do not require anchoring and are both economically and technically possible.[10] Reinforcement with fiber can be applied for stabilizing subgrade soils in road construction, in sands and different kinds of clays. Fiber-reinforcement was found to increase the passes number to failure in road tests.[11] Increasing the shear strength of the backfill materials by fiber reinforcement, the amount planar reinforcement requirement will be minimized and at the same time it may minimize the necessity for strengthening material. For reinforced slopes or walls, planar geosynthetics can be used with fiber reinforcement together.[12] To evaluate the influence of fibers on stability, soil structures reinforced with randomly distributed fibers are generally generated using composite methods. The mixture is treated as a homogeneous composite material in these conditions. The role of fibers is previously studied using friction angle and soil cohesion. Several studies were discussed composite models for a better understanding of fiber behavior inside the soil. Mechanical,[5] statistical,[13] and an energy-based limit analysis models are some of them.[14]

Horizontal fiber reinforcement is a common method for subgrade reinforcement. The spacing and direction of reinforcing can lead to weak interfaces, causing only lateral subgrade deformation to be managed while the problem of subgrade settlement deformation remains uncontrolled. As a solution, 3D (three-dimensional) fiber reinforcement has been introduced for subgrade projects. This fiber reinforcing method is a technique used in geotechnical composite preparation that incorporates short or continuous fibers into the soil in a random and discontinuous manner.[15] It is feasible to increase soil strength properties through friction between the soil and fiber as well as friction between the fibers in the 3D reticulated fiber system.[16,17] In the study by Botero *et al.* (2105), triaxial shear tests were doneto study the mechanical characteristics of recycled PET (Polyethylene terephthalate) fiber-reinforced silt, and it was discovered that the fibers improved the soil's resistance to deformation.[18] According to researchs, fiber characteristics, properties of soil, and other

external factors all influence the fiber-reinforced soil strength, with fiber content having the greatest impact.[19,20] According to researchs, the stress-strain behaviour of soil reinforced with fiber did not differ from that in unreinforced soil and still showed strain-hardening characteristics.[21,22]

The influence of fiber incorporation on the fill's mechanical properties revealed that increasing of cohesiveness of soil (0 to 0.11 Mpa), lead to a decrease in the internal friction angle (38° to 37.7°). The increase in cohesion was even more noticeable with fiber incorporation when compared to the change in internal friction angle.[22–24] In different studies, the effect of fiber content was studied, and it was found that the optimal fiber content used for reinforcing cohesive soils such as clays or silts depends on parameters such as fiber type, soil properties, and particle size. This content is mostly in the range of 0.1% to 0.3%. For granular soils, fiber content can be more than the above range.[25,26] Xiangwei *et al.* (2020) studied coral sand that was reinforced with microbially induced calcite precipitation (MICP). The engineering characteristics of samples were tested in this study, and the results showed that MICP decreased permeability and increased unconfined compressive strength. Additionally, while studying the the engineering properties, the effect of the fiber content of MICP-treated coral sand was greater than the fiber length. Fiber physical properties will affect the reinforcement results too.[27] Zhao *et al.* (2021) investigated the effects of different fibers on calcareous sand. In this research, the small-strain dynamic properties of calcareous sand reinforced with hemp MICP and polyester mixture were studied. According to the results, hemp fiber with a rougher surface led to a greater damping ratio in samples.[28]

Reinforcing of soil can affect the movement of aggregate particles. This can have an impact on settlement, shear failure surfaces, load distribution, and load transfer to subsoil layers. While the soil is forming two different layers, the soil failure mechanism will change. As seen in Fig. 1, it showes two-layer soil with a stronger layer at the top and a weaker one at the bottom, with failure zones of soil under strip footing. When the depth of the stronger layer is not enough, some parts of failure zones will occur in the second layer. This behaviour of different layyers can occur not only under footings but in other cases too. Ahmadi & Hajialilue (2012) presented a logarithmic spiral failure surface originating from the wall base for retaining structures in an active state.[29]

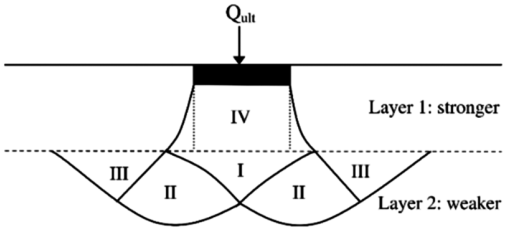

Fig. 1 — Failure mechanism of two layers soil underlying a strip footing[29]

Movements of soil mass can be investigated or even analyzed with experimental and numerical modeling. In a laboratory, different thin layers can be located inside soil to see the movement of soil mass under loading. Another better method is using PIV (Particle Image Velocimetry) methods. By taking high-resolution pictures during the experimental tests, settlement of footing or movement of aggregates can be obtained by processing the pictures.[30,31] In numerical modeling for estimating bearing capacity, shear failure surfaces, and movement of soil, Different Finite Element (FEM), Discrete Element (DEM), or other methods can be used.

The current study's main objective is to evaluate the optimal reinforced depth and depth-bearing capacity of randomly polypropylene fiber-reinforced sandy soil to improve the discrete framework for soil reinforcement and provide a better understanding of the behavior and mechanical properties of fiber-reinforced soil. This study includes the experimental testing program. The soil, with two relative densities of 50% and 65%, was randomly reinforced with fiber. Unreinforced and reinforced soil samples were tested by loading under a strip footing in a model tank. The depth of reinforcement differed from B to 3B (where B is the model strip footing width). The behavior of unreinforced and reinforced soil was investigated and analyzed by the Geo-PIV method at different s/B ratios (s is the settlement of footing) and experimental results of shear failure surfaces were compared with the results of the finite element method (FEM) to find the optimal reinforcing depth of soil under strip footing. The results can be used in real engineering applications as optimum reinforcing depths to design and construct economic structure.

Materials and Methods

Soil

The sand used for this study was obtained from the Birkum sand quarry that is 5 km away from Erzurum (39.84945, 41.18591). It was moved, washed, and

dried in the laboratory at room temperature. The soil was sieved through 2 mm in diameter (No. 10) and 500 μm diameter (No. 35) sieves according to ASTM D6913-04 standard. According to the Unified Soil Classification Systems (USCS) standard (ASTM D2487-17), the soil is classified as poorly graded sand (SP) with uniformity coefficient value of C_u=2.21 and curvature coefficient value of C_c = 80. The grain size distribution of soil used for preparing samples is shown in Fig. 2.

According to ASTM D854, the specific gravity of the sand used was determined by the pycnometer test and found to be Gs = 2.67 that means the sand is classified as normal or silty sand range. Soil samples were prepared at two relative densities (Dr) of 50% and 65%. For preparing samples at the mentioned relative densities, the maximum and minimum unit weights of the sand used in the experiments were determined according to ASTM D4253-16e1 and ASTM D4254-16 standards. By doing a direct shear test, the friction angle of soil at relative densities of 50% and 65% was obtained as 40° and 46°, respectively. The mechanical properties of soil were shown in Table 1.

Table 1 — Mechanical properties of soil

Mechancal properties of soil	
Soil Classification (USCS)	SP
D_{10} (mm)	0.67
D_{30} (mm)	1.48
D_{60} (mm)	2.21
$Cu = D_{60}/D_{10}$	2.21
$Cc = (D_{30})^2 / (D_{60}.D_{30})$	80
Specific Gravity	2.67
Minimum Void Ratio	0.52
Maximum void Ratio	0.84
Friction Angle at Dr=50%	40°
Friction Angle at Dr=65%	46°

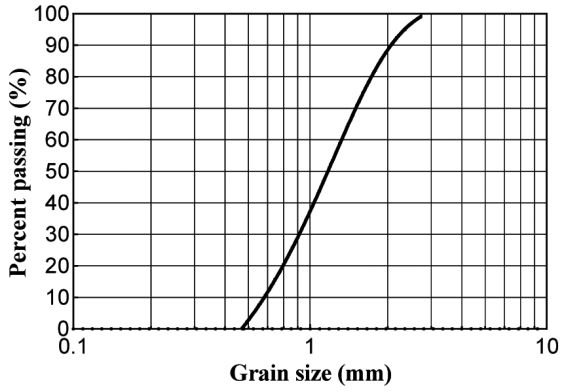

Fig. 2 — Grain Size distribution of Soil

Polypropylene Fiber

In the tests, wavy polypropylene bristles boughted from industry and cutted with a length of 20 mm and used as reinforcement. The tensile strength of the fibers was determined as 150 MPa and the density as 9 kN/m^3. The polypropylene fiber used is shown in Fig. 3(c).

The volumetric fiber content is calculated using the following equation[32] (Eq. 1):

$$X = \frac{V_f}{V} \quad \ldots (1)$$

in which, V is the fiber-soil composite control volume and V_f is the volume of fibers. The gravimetric fiber content (Y), which is commonly used in constructing specifications, can be defined as[19]:

$$Y = \frac{W_f}{W_s} \quad \ldots (2)$$

where, W_s and W_f denote dry weight of soil and weight of fibers respectively. The dry unit weight of fiber-reinforced soil (γ_d) can be calculated as follow[32]:

$$\gamma_d = \frac{W_f + W_s}{V} \quad \ldots (3)$$

and by considering previous equation the relationship between X and Y can be as below[32]:

$$X = \frac{Y.\gamma_d}{(1+Y).G_f.\gamma_w} \quad \ldots (4)$$

that γ_w is unit weight of water and G_f is specific gravity of fiber used as reinforcement. The aspect ratio describes the geometry of fiber, which is defined as:

$$\eta = \frac{l_f}{d_f} \quad \ldots (5)$$

that l_f and d_f are length and equivalent diameter of fiber respectively.

Model Tank

Model plate loading tests on sandy soil were carried out with and without reinforcement. A rigid polyamide model foundation with a width of B = 50

Fig. 3 — Different components of model tank: (a) Model Strip Footing, (b) Model Tank, (c) Fibers

mm, a height of H = 40 mm and a length of L = 100 mm was used in the laboratory tests for modeling a strip footing (Fig. 3a).[30,31] The parameters affecting the bearing capacity of continuous foundations resting on polypropylene fiber-reinforced sandy soil were investigated experimentally. During the tests, two displacement meters (LVDT) were placed at the two corners of the foundation plate to check its settlement. If the two LVDT readings differed from each other, the experiments were repeated because they did not fulfill the central loading conditions. The test tank was formed with dimensions of 100 cm (length), 10 cm (width), and 100 cm (height). Its front face is made of 20 mm thick fiberglass, and its rear and side surfaces are made of 5 mm steel sheet. In addition, the test tank is supported by boxes and L shape profiles to prevent deformation of tank. In order for the soil to be emptied easily, a discharge chamber is made at the bottom of the tank.[30,31] The model tank and strip footing are shown in Fig. 3b.

Loading System: In the experiments, a 5000 kg capacity hydraulic jack with adjustable loading speed was used to load the model footing at a constant speed, and a load cell was used to determine the loads on the foundation plate. The values taken from the load cells and LVDTs were transferred to the 8-channel data acquisition device. Before starting the tests, each sensor was calibrated. The main function of the data collection device is to convert the slowly changing static or semi-static signals from the sensors into digital data and transfer them to the computer environment.

Digital Camera: In the study, successive photographs were taken every 30 seconds with a camera with a resolution of 3264 × 1836 fixed on a tripod without any movement. The resulting photographs were analyzed with the program Geo-PIV8, and the deformations on the sandy ground were observed.[33]

The optimum bearing depth relationship of the strip foundation on a medium-density sandy soil with and without reinforcement was investigated by laboratory tests. Unreinforced tests were carried out first, and then reinforced tests were done. In the unreinforced tests, the relative density of soil was chosen at 50% and 65%. In order to provide the desired relative firmness, the sand soil was placed in the tank in layers of 10 cm. The amount of reinforcement used was 1% of the weight of the sand in the tank. In the reinforced sample tests, reinforced soil was placed from the bottom of the foundation plate to the depths of B, 2B, 2.5B, and 3B (B is the width of the footing). After compaction, the horizontal straightness of the upper surface of the foundation plate was checked with a spirit level, and the model strip footing was placed on a flat soil surface. To ensure the results, each test was repeated at least 3 times. The constant loading speed used for all tests is 1 mm/min. The friction between the footing and the glass surfaces is neglected. All instrument readings were reset before starting the tests. In all the tests, data was recorded every 10 seconds from the LVDTs and the load cell. The settlement of the foundation plate and the central loading condition were checked with displacement meters placed at the two corners of the footing. The tests were repeated when different settlements occurred in the footing during the experiment, that is, if the central loading condition could not be met.

Particle Image Velocimetry (PIV) Method

The PIV method is a flow-free areal velocity measurement method and is used for the examination of flow in many branches. White *et al.* (2003) made some changes to the PIV technique and made it suitable for studies in the field of geotechnical engineering. Thus, it has become possible to define and evaluate the deformations of soils.[33,34] Geo-PIV is a MATLAB module that can measure velocity with particle images in accordance with geotechnical tests. It is used to measure displacement fields from digital images. In this study, the PIV method was used to observe and describe the deformations that occur in an unreinforced and randomly reinforced with polypropylene fiber sand under a shallow strip foundation. During the tests, photographs were taken at 30-second intervals with a high-resolution camera. The camera is fixed in order to prevent minor vibrations that may occur during photographing. The resulting photographs were analyzed with the program Geo-PIV8 and the deformations in the sandy soil were observed.[34] The program creates a mesh for the selected area. The Geo-PIV8 algorithm then searches for the first tile in the next photograph taken in motion and obtains the motion vector as soon as it achieves the highest similarity. Thus, motion vectors are obtained. Since each sand has a unique structure, there is no need to use target particles in the PIV method. This feature is one of the most important advantages of this method.[34]

Unreinforced and randomly polypropylene fiber-reinforced, poorly graded sand were subjected to model loading tests. The sand was placed at two different relative densities of 50% and 65% in the

model tank. For each relative density, the placed soil was reinforced at different depths. At the next step, a model strip footing was loaded. Plate loading test results for strip footing on medium-density sandy soil with and without reinforcement are investigated. The behavior of soil and shear failure surfaces was investigated by taking pictures every 30 seconds and analyzing them with Geo-PIV8. At the same time, the effect of reinforcement was calculated by stress-deformation graphs at different conditions. In the next step, shear failure surfaces were investigated by FEM modeling and the results were compared with experimental results gained from the PIV method.

Work Design/Program

First, unreinforced tests were carried out without using polypropylene fiber. Sand with relative densities of 50% and 65% was placed in the model tank and tested. Loading was done at a speed of 1 mm/min with the help of a hydraulic jack. With the aid of two LVDTs placed diagonally, the settlement of the foundation plate was observed. In the unreinforced test models, the average base pressure-settlement curves were obtained as a result of the loading tests. In the unreinforced tests, the ultimate bearing capacity at the time of the formation of the slip surfaces was determined as an average of qu = 52 kPa for Dr = 50% and an average of q_u = 172 kPa for Dr = 65%. Terzaghi (1943) defined the ultimate bearing capacity for strip foundations resting on sandy soils.[35] It is indicated by the expression $q_u = 0.5\gamma B N\gamma$. The ultimate bearing capacity obtained from the Terzaghi bearing capacity theory was determined as q_u = 46 kPa for Dr = 50% and q_u=167 kPa for Dr = 65%. It is seen that the experimental and theoretical results are in good agreement with each other. The results obtained from the tests carried out by adding polypropylene fibers at different depths to the sand sample of different relative densities are given. All parameters used in the experiments were determined by scanning the literature. In the research, average base pressure-settlement curves and bearing capacity ratios were examined. The carrying capacity ratio is defined as follows:

$$BCR = \frac{q}{q_u} \quad \ldots (6)$$

Here, BCR is the bearing capacity ratio, q is the reinforced mean base pressure, and q_u is the unreinforced mean base pressure. While determining the BCR values, the mean base pressure-settlement curves of the reinforced tests were examined. Since the settlements are relatively large, comparisons were made in terms of bearing capacities corresponding to a certain settlement ratio (s/B). In addition, the final bearing capacities were determined by intersecting the tangents taken from the start and end points of the mean base pressure-settlement curves in the reinforced tests.

Results and Discussion

Constant Relative Density and Different Reinforcement Depths Behavior

The depth of reinforcement was changed and average base pressure-settlement plots were obtained for soil with Dr = 50% and 65% and the results are presented at Fig. 4. As seen in Fig. 4, the bearing pressure of soil increased by increasing the reinforcement depth in both soils with Dr = 50% and Dr = 65%. At the same time, in soil with Dr = 50% increasing the reinforcing depth changed the behavior of soil mass such that, by considering the Settlement-Bearing Pressure graphs, it moved from punching shape toward local shear failure. On the other hand, in samples with Dr = 65%, the behavior of soil moved from local toward a general shear failure mechanism

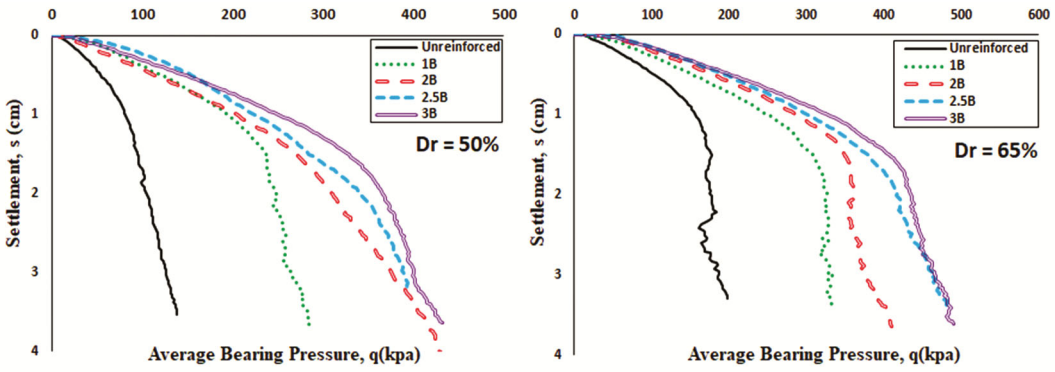

Fig. 4 — Average base pressure-settlement curves at different reinforcing depths (Dr = 50%)

that shows the effect of reinforcing depth on total soil mass behavior. The reason for these changes can be explained by the effect of reinforcement. Improving the upper layer will lead to transferring the load to deeper layers, and the effect of soil reinforcement will act like increasing the depth of footing.

On continue, Fig. 5 shows the "reinforcement depth-carrying capacity ratio" relation corresponding to different settlement ratios and the "settlement ratio-bearing capacity ratio" relationship corresponding to the use of reinforcement at different depths. By considering this figure, it shows that increasing reinforcing depth will lead to an increasing BCR ration in different s/B ratios in both soils with relative densities of 50% and 60%. In just soil with Dr = 50%, the BCR ratio increased up to s/B = 0.3 and after that, the amount of BCR started to decrease.

For different reinforcement depths, "the settlement ratio-bearing capacity ratio" graphs were presented in Fig. 6. In this figure, soil with different relative densities of 50% and 65%, BCR was shown at different s/B ratios and different reinforcing depths. For all test conditions, the bearing capacity increased with increasing reinforcement depth or relative density of soil. By considering the graphs, it was found that the behavior of soil under strip footing loading changes by changing the relative density of soil. This is more noticeable when the reinforcing depth is equal to B.

Generally, the BCR-increasing manner was changed to s/B = 0.3 in soils with a relative density of 50%. For s/B ratios greater than 0.3, the increase in value of BCR started to decrease or the increasing ratio was decreased. But in soils with Dr = 65%, the value of BCR was continuing its increasing behavior in all s/B ratios.

At Dr = 50%, a significant increase in bearing capacity up to 2B reinforcement depth and a decrease in settlements at the same base pressure were observed. However, if the reinforcement depth is greater than 2B, the increase in bearing capacity and the decrease in settlements corresponding to the same base pressure did not change much. At a constant settlement ratio (s/B), the BCR value increased as the reinforcement depth increased. By considering the BCR equation, by increasing the reinforcement depth, the reinforced mean base pressure (q) will be increased that lead to increasing the BCR ratio. for For example,

- If s/B = 0.1, BCR=2.2 at B reinforcement depth and BCR = 2.7 at 3B reinforcement depth.
- If s/B = 0.2, BCR = 2.4 at B reinforcement depth and BCR = 3.0 at 3B reinforcement depth.
- In case of s/B = 0.3, BCR = 2.5 at B reinforcement depth and BCR = 2.9 at 2B reinforcement depth.

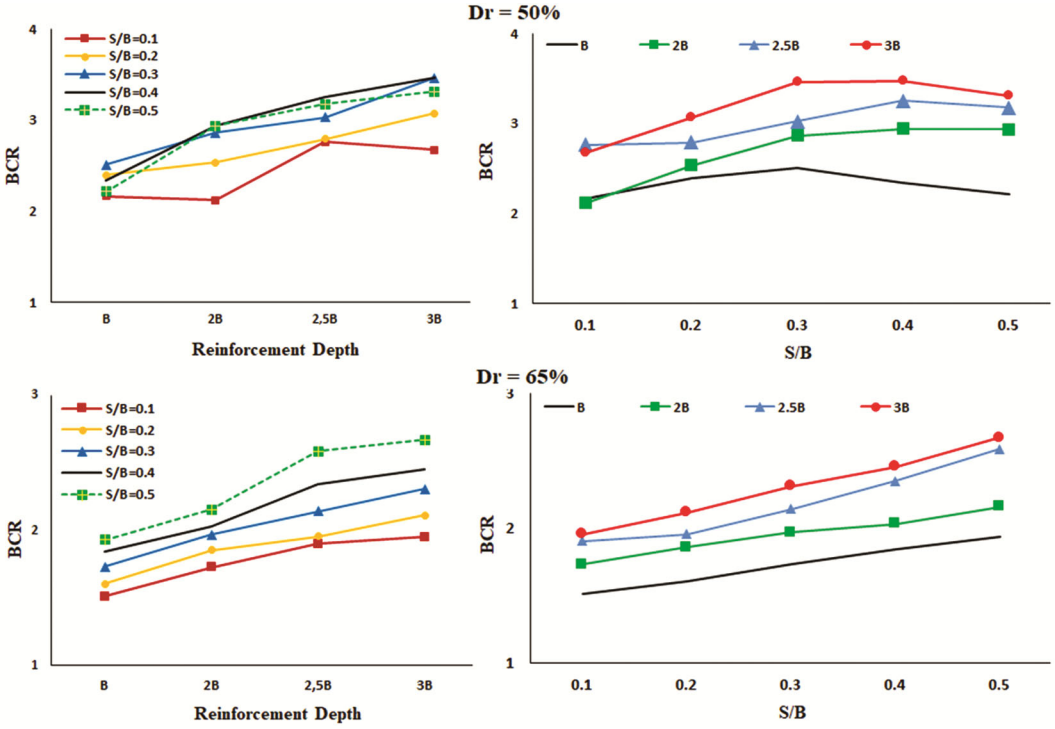

Fig. 5 — Reinforcement depth-BCR and s/B-BCR relationship corresponding to different settlement ratios and reinforcement depths

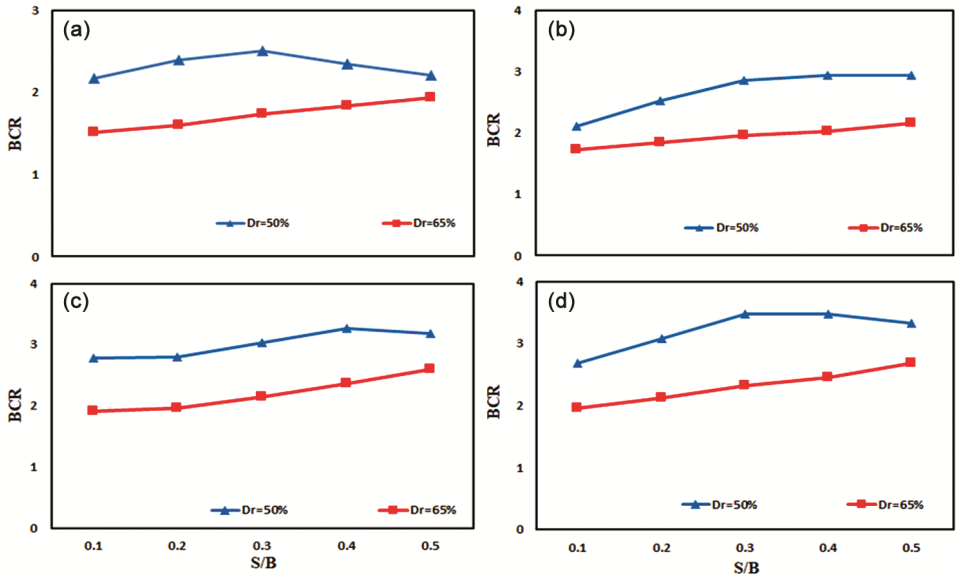

Fig. 6 — Change in settlement ratio-BCR in different reinforcing depths and relative densities

The value of BCR increased as the settlement rate increased at constant reinforcement depth. For example,

- In the case of B reinforcement depth, BCR = 2.2 corresponding to the ratio of s/B = 0.1, whereas BCR = 2.4 at s/B = 0.2.

- In the case of 2B reinforcement depth, BCR = 2.1 corresponding to the ratio of s/B = 0.1, whereas BCR = 2.9 at s/B = 0.5.

- In the case of 3B reinforcement depth, BCR = 3.1 corresponding to the ratio of s/B = 0.2, whereas BCR = 3.3 at s/B = 0.5.

For tests on soil with Dr = 65%, the ultimate bearing capacity increased as the reinforcement depth increased and decreased proportionally at the same base pressure value. As the reinforcement depth increased, the slope of the initial part of the base pressure-settlement curve decreased. A significant increase in bearing capacity up to a reinforcement depth of 2.5B and a decrease in settlements at the same base pressure were observed. However, if the reinforcement depth is greater than 2.5B, the increase in bearing capacity and the decrease in settlements corresponding to the same base pressure did not change much.

At a relative density of 65%, at a constant settlement ratio (s/B), the BCR value increased as the reinforcement depth increased. For example,

- If s/B = 0.1, BCR = 1.5 at B reinforcement depth and BCR = 2.0 at 3B reinforcement depth.

- In case of s/B = 0.2, BCR = 1.9 at 2B reinforcement depth and BCR = 2.1 at 3B reinforcement depth.

- In case of s/B = 0.5, BCR = 1.9 at B reinforcement depth and BCR = 2.6 at 2.5B reinforcement depth.

The BCR increased while the settlement ratio increased at constant reinforcement depth. For example,

- In the case of 2B reinforcement depth, BCR = 1.7 corresponding to the ratio of s/B = 0.1, whereas BCR = 2.0 at s/B = 0.3.

- In the case of reinforcement depth of B, BCR = 1.5, corresponding to the ratio of s/B = 0.1, whereas BCR = 1.9 at s/B = 0.5.

- In case the reinforcement depth is 2.5B, BCR = 2.1 corresponding to the ratio of s/B = 0.3, whereas BCR = 2.6 at s/B = 0.5.

In the case of B of depth reinforcement (B), the BCR decreased as the relative stiffness increased at the fixed settling ratio. e.g.

- BCR = 2.2 at 50% relative density at s/B = 0.1, while BCR = 1.5 at 65% relative density.

- BCR = 2.4 at 50% relative density at s/B = 0.2, while BCR = 1.6 at 65% relative density.

- BCR = 2.2 at 50% relative density at s/B = 0.5, while BCR = 1.9 at 65% relative density.

In contrast to the reinforcement depth of B, in the case of using reinforcement of 2B, the BCR increased as the s/B ratio increased at constant relative stiffness. For example,

- At Dr = 50%, BCR = 2.1 at s/B = 0.1 and BCR = 2.9 at s/B = 0.5.

- At Dr = 50%, BCR = 2.5 at s/B = 0.2 and BCR = 2.9 at s/B = 0.3.
- At Dr = 65%, BCR = 1.7 at s/B = 0.1 and BCR = 2.2 at s/B = 0.5

At the same time, BCR increased as the s/B ratio increased at constant relative stiffness. For example,

- At Dr = 50%, BCR = 2.2 at s/B = 0.1 and BCR = 2.5 at s/B = 0.3.
- At Dr = 65%, BCR = 1.6 at s/B = 0.2 and BCR = 1.9 at s/B = 0.5.
- At Dr = 65%, BCR = 1.5 at s/B = 0.1 and BCR = 1.7 at s/B = 0.3.

For Dr = 50%, if the reinforcement depth is greater than 2B, the increase in bearing capacity and the decrease in settlements corresponding to the same base pressure did not change by a considerable amount. At a constant settlement ratio (s/B), the BCR value increased as the reinforcement depth increased. For example, if s/B = 0.2, BCR = 2.4 at B reinforcement depth and BCR = 3 at 3B reinforcement depth. The BCR increased as the settlement ratio (s/B) increased at 50% relative density at constant reinforcement depth.

In the both cases of 2.5B and 3B reinforcements, the BCR value increased as the s/B ratio increased at constant relative density. For example,

- At Dr = 50%, BCR = 2.8 at s/B = 0.2 and BCR = 3.0 at s/B = 0.3.
- At Dr = 50%, BCR = 3.1 at s/B = 0.2 and BCR = 3.5 at s/B = 0.3.
- At Dr = 50%, BCR = 2.8 at s/B = 0.1 and BCR = 3.2 at s/B = 0.5.
- At Dr = 50%, BCR = 2.7 at s/B = 0.1 and BCR = 3.3 at s/B = 0.5.
- At Dr = 65%, BCR = 2.0 at s/B = 0.1 and BCR = 2.7 at s/B = 0.5.
- At Dr = 65%, BCR = 1.9 at s/B = 0.1 and BCR = 2.6 at s/B = 0.5

and the BCR decreased as the relative density increased at the fixed settlement rate.

- BCR = 2.7 at Dr = 50% at s/B = 0.1 settlement ratio, while BCR = 2.0 at Dr = 65%.
- BCR = 3.1 at Dr = 50% at s/B = 0.2 settlement ratio, while BCR = 2.1 at Dr = 65%.
- BCR = 3.3 at Dr = 50% at s/B = 0.5 settlement ratio, while BCR = 2.7 at Dr = 65%.

For Dr = 50%, a significant increase in bearing capacity up to 2B reinforcement depth, and a decrease in settlements at the same base pressure were observed. For Dr = 65%, a significant increase in bearing capacity up to a reinforcement depth of 2.5B and a decrease in settlements at the same base pressure were observed. However, if the reinforcement depth is greater than 2.5B, the increase in bearing capacity and the decrease in settlements corresponding to the same base pressure did not change much. At a constant settlement ratio (s/B), the BCR value increased as the reinforcement depth increased. For example, if s/B = 0.5, the BCR = 1.9 at B reinforcement depth and BCR = 2.6 at 2.5B reinforcement depth.

Particle Image Velocity Analysis

In this section, the PIV method was used to observe the formation of a slip surface, which is a result of the deformation behavior up to the collapse point, as a result of tests performed by adding reinforcement at different depths to a sand sample of different relative density under a strip foundation. The Geo-PIV8 software running under the MATLAB R2013B program was used to observe the formation of the results. Slippages in the soil under model strip footing were analyzed with the PIV method when the foundation was settled by 1 cm (s/B = 0.2) and 2 cm (s/B = 0.4) at unreinforced samples and different reinforcement depths with two relative densities of Dr = 50% and Dr = 65%. Results of PIV method were obtained and presented in Figs 7 & 8. They show the shear failure surfaces of soil with Dr = 50% and Dr = 65% respectively, under strip footing with different reinforcement depths and settlement values.

From PIV results, it showed that, by increasing the reinforcement depth, the slip band stays higher. In other words, as the reinforcement depth increases, the soil depth affected by the foundation pressure decreases. It was observed that the movement of soil grains was greater in unreinforced tests. As the settlement increased, the affected depth area of soil under footing and shear failure surfaces also increased toward subsoil areas. Based on the Geo-PIV results, the lateral movement of the soil under footing decreased with the increase of reinforcement depth. Spiral-shaped slip bands were observed, especially in unreinforced modeling (Fig. 9).

Finite Element (FEM) Analyzing

To compare the results obtained from the PIV method, finite element modelling was done to understand soil behaviour and movement under strip footing in different unreinforced and reinforced soils. Here, the main purpose of modelling was to better

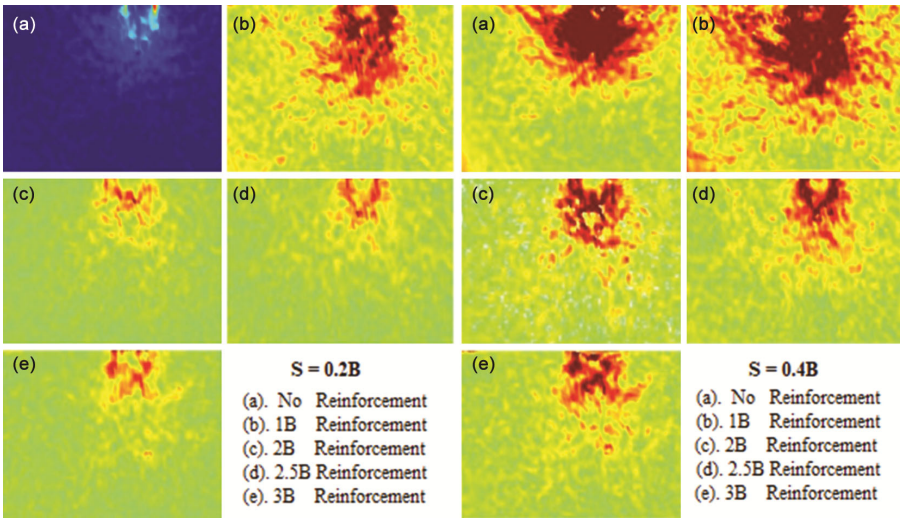

Fig. 7 — Shear failure surfaces for different reinforcement depths using the PIV method (s = 0.2B and s = 0.4B, Dr = 50%)

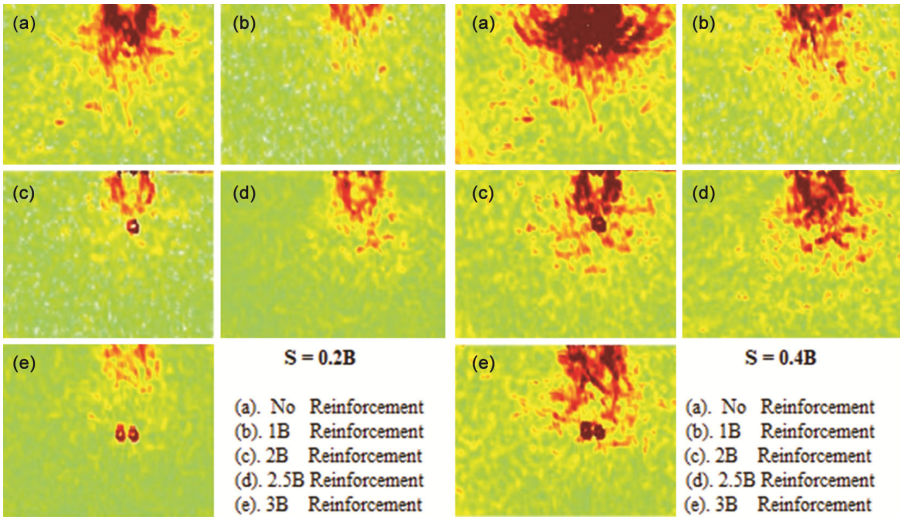

Fig. 8 — Shear failure surfaces for different reinforcement depths using the PIV method for Dr = 65%

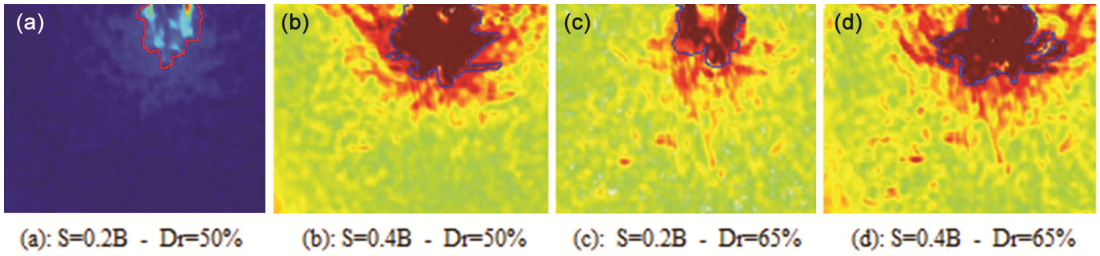

Fig. 9 — Spiral-shaped slip bands in unreinforced samples

understand soil behavior at different conditions of settlement and reinforcing. As seen in Figs 10 & 11 varied by relative densities (Dr), by increasing the reinforcement depth, the failure mechanism of soil moves to deeper layers and the main displacement of aggregate happens in stronger layers. Generally, in the condition of 3B depth of reinforcement, there is no more displacement or movement in normal unreinforced layers. In just 2.5B of reinforcements, there are some movements in deeper areas of soil, but the amount of this movement is negligible. In both experimental and numerical modelling, the lateral

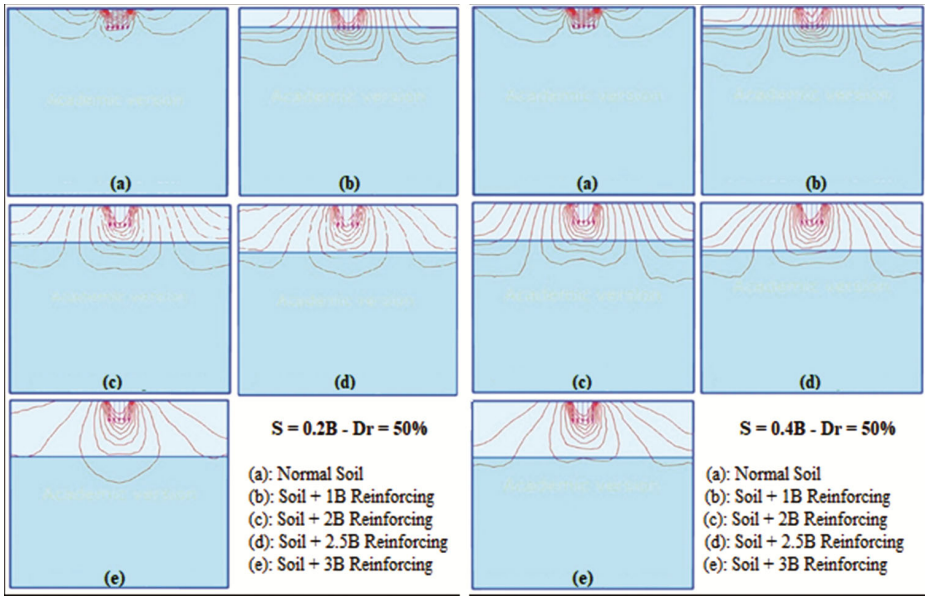

Fig. 10 — Results of FEM modelling for soils with Dr=50% in different unreinforced and reinforced conditions in two different s/B ratios of 0.2 and 0.4

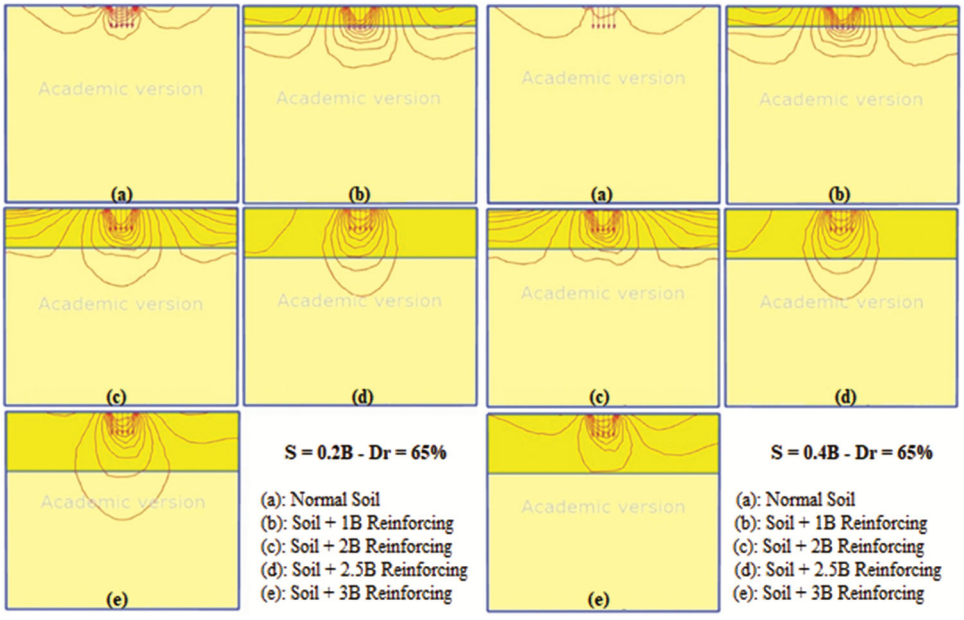

Fig. 11 — Results of FEM modelling for soils with Dr = 60% in different unreinforced and reinforced conditions in two different s/B ratios of 0.2 and 0.4

movement of soil on the right and left sides of the footing decreased by increasing the reinforcement depths. It is because of transferring the load toward deeper layers that the shear failure mechanism of soil is changing by increasing the reinforcement depth.

As seen in these figures, the effect of reinforcing shows itself by transferring the loads and displacement toward the lower layers. By looking at the results of the PIV and FEM methods, it was found that in unreinforced soil samples, lateral movements are more considerable under strip footing settlement than in different layers of soil reinforced under footing. At 1B or 2B depth of reinforcing, the movement of soil aggregate is seen on both the right and left side of the soil at the same time under the footing. But the heaving of soil on the left and right sides of the footing is less than the unreinforced condition. By increasing the reinforcing depth to

2.5B, lateral movements decrease considerably, and displacement occurs more in the vertical direction than in the horizontal. Because of this, the area under footing is more critical than other areas. At this condition, some parts of the movement and effect depth are in reinforced layers and some parts are in lower unreinforced layers. While the reinforcement depth increased to 3B, the main movement happened under the footing and in the reinforced layer. Unreinforced layers were not affected by footing settlement so much in 3B of reinforcement depth. Both PIV and FEM modeling show the same behavior in the movement of aggregate. These findings are in agreement with the findings in the literature. For example, at the study of Jahanger *et al*., (2018) placing a strong layer on a weaker granular soil lead to failure surfaces moved toward deepr layer. Other studies shows the same results.[29,36,37]

Conclusions

For both relative densities of 50% and 65%, the ultimate bearing capacity increased when the depth of reinforcement increased and settlements decreased at the same base pressure value. For Dr = 50%, a significant increase in bearing capacity up to 2B reinforcement depth, and a decrease in settlements at the same base pressure were observed. For Dr = 65%, a significant increase in bearing capacity up to 2.5B reinforcement depth and a decrease in settlements at the same base pressure were observed. The amount of BCR increased as the settlement ratio increased at constant reinforcement depth. Based on results, in soil with medium densities (Dr = 50%) the optimal reinforcement depth can be selected as 2B while at Dr = 65%, the reinforcement depth can be selected up to 2.5B, depending on the final purpose of improvement. Selecting the depth of 3B for reinforcing will not be so economical while the differences between 3B and 2B or 2.5B of reinforcements will not be considerable. The 2B or 2.5B of reinforcement depth, depending on soil density and purpose of reinforcing will give better results than the 1B or 3B.

Acknowledgments

The authors thank Ataturk University for providing the geotechnical laboratory, materials, and experimental setups. At the same time, the authors thank Erzurum Technical University for preparing the Plaxis software for numerical modelling of this research.

References

1 Okonta F N & Ojuri O O, The stabilization of weathered dolerite aggregates with cement, lime, and lime fly ash for pavement construction, *Adv Mater Sci Eng*, **2014** (2014) 11 pages, https://doi.org/10.1155/2014/574579

2 Naghizadeh A & Ekolu S O, Effects of compositional and physico–chemical mix design parameters on properties of fly ash geopolymer mortars, *Silicon*, **13(12)** (2021) 4669–4680, https://doi.org/10.1007/s12633-020-00799-2

3 Naghizadeh A & Ekolu S O, Activator - related effects of sodium hydroxide storage solution in standard testing of fly ash geopolymer mortars for alkali – silica reaction, *Mater Struct*, **55(22)** (2022) 1–16, https://doi.org/10.1617/s11527-021-01875-8

4 Wu T H, Beal P E & Lan C, In situ shear test of soil-root system, *J Geotech Eng, ASCE*, **114(12)** (1988) 1376–1394.

5 Gray D H & Ohashi H, Mechanics of fiber-reinforcement in sand, *J Geotech Eng*, *ASCE*, **109(3)** (1983) 335–353.

6 Al-Refeai T O, Behavior of antigranulocytes soils reinforced with discrete randomly oriented inclusions, *Geotex Geomemb*, **10(4)** (1991) 319–333.

7 Zornberg J G, Peak versus residual shear strength in geosynthetic-reinforced soil design, *Geosynth Int*, **9(4)** (2002) 301–318, https://doi.org/10.1680/gein.9.0220

8 Murray J J, Frost J D & Wang Y, Behavior of a sandy silt reinforced with discontinuous recycled fiber inclusions, *Transp Res Rec*, **1714** (2000) 9–17.

9 Consoli N C, Montardo J P, Prietto P D M & Pasa G S, Engineering behavior of a sand reinforced with plastic waste, *J Geotech Geoenviron Eng*, *ASCE*, **128(6)** (2002) 462–472.

10 Zornberg J G, Somasundaram S & LaFountain L, Design of geosynthetic-reinforced veneer slopes, *Proc Int Symp Earth Reinforcement (IS Kyushu 2001*, Tokyo, Japan) **1**, 2001, 305–310.

11 Santoni R L, Tingle J S & Webster S L, Engineering properties of sandfiber mixtures for road construction, *J Geotech Geoenviron Eng*, *ASCE*, **127(3)** (2001) 258–268.

12 Gregory G H, Reinforced slopes using geotextile-fiber composite,*Proc*, *30thAnnual Southeastern Transport Geotech Eng Conf*, Louisville, KY, 1998.

13 Ranjan G, Vasan R M & Charan H D, Probabilistic analysis of randomly distributed fiber-reinforced soil, *J Geotech Eng*, *ASCE*, **122(6)** (1996)419–426.

14 Michalowski R L & Zhao A G, Failure of fiber-reinforced granular soils, *J Geotech Eng*, *ASCE*, **122(3)** (1996) 226–234.

15 Bao C & Ding J, Researches and applications of fiber reinforced soils, *Soil Eng Found*, **26** (2012) 80–83.

16 Liu B, Tang C, Li J, Wang D, Zhu K & Tang W, Advances in engineering properties of fiber reinforced soil, *J Eng Geol*, **21** (2013) 540–547.

17 Shao W, Cetin B, Li Y, Li J & Li L, Experimental investigation of mechanical properties of sands reinforced with discrete randomly distributed fiber, *Geotech Geol Eng*, **32** (2014) 901–910.

18 Botero E, Ossa A, Sherwell G & Ovando-Shelley E, Stress–strain behavior of a silty soil reinforced with polyethylene terephthalate (PET), *Geotext Geomembr* **43(4)** (2015) 363–369, https://doi.org/ 10.1016/ j.geotexmem.2015.04.003.

19 Plé O & Lê T N H, Effect of polypropylene fiber-reinforcement on the mechanical behavior of silty clay,

Geotext Geomembr, **32** (2012) 111–116, https://doi.org/10.1016/j.geotexmem.2011.11.004.

20 Cristelo N, Cunha V M C F, Dias M, Gomes A T, Miranda T & Araújo N, Influence of discrete fibre reinforcement on the uniaxial compression response and seismic wave velocity of a cement-stabilised sandy-clay, *Geotext Geomembr*, **43** (2015) 1–13, https://doi.org/10.1016/j.geotexmem.2014.11.007.

21 Machado S L, Vilar O M & Carvalho M F, Constitutive model for long term municipal solid waste mechanical behavior, *Comput Geotech*, **35** (2008) 775–790.

22 You B, Xu H & Dong J, Triaxial tests of expansive soil reinforced with basalt fiber, *J Disaster Prev Mitig Eng*, **35** (2015) 503–507-514.

23 Kutara K, Miki H, Horiya S, Ishizaki H & Fujiki H, Mechanical behavior of reinforced soil by continuous threads, *Proc Geotext Symp*, **3** (1988) 27–33.

24 Wang D, Tang C, Li J, Liu B, Tang W & Zhu K, Shear strength characteristics of fiber-reinforced unsaturated cohesive soils, *Chin J Geotech Eng*, **35** (2013) 1933–1940.

25 Wang P, Tang C, Sun K, Chen Z, Xu S & Shi B, Experimental investigation on consolidation properties of fiber reinforced municipal sludge, *J Eng Geol*, **23** (2015) 687–694.

26 Prabakar J & Sridhar R S, Effect of random inclusion of sisal fibre on strength behaviour of soil, *Constr Build Mater*, **16** (2002) 123–131.

27 Xiangwei F, Yang Y, Zhe C, Hanlong L, Yang X & Chunni S, Influence of fiber content and length on engineering properties of mıcp-treated coral sand, *Geomicrobiol J*, **37(6)** (2020) 582–594, DOI: 10.1080/01490451.2020.1743392

28 Zhao J, Tong H, Shan Y, Yuan J, Peng Q & Liang J, Effects of different types of fibers on the physical and mechanical properties of mıcp-treated calcareous sand, *Materials (Basel)* **7**, **14(2)** (2021) 268, doi: 10.3390/ma14020268, PMID: 33430360, PMCID: PMC7825789.

29 Ahmadi H & Hajialilue-Bonab M, Experimental and analytical investigations on bearing capacity of strip footing in reinforced sand backfills and flexible retaining wall, *Acta Geotech*, 7 (2012) 357–373, https://doi.org/10.1007/s11440-012-0165-8

30 Çelik S, Ghalehjough B K, Majedi P & Akbulut S, Effect of randomly fiber reinforcement on shear failure surface of soil behind flexible retaining walls at different conditions, *Indian J Mar Sci*, **46** (2017) 2097–2104.

31 Ghalehjough B K, Akbulut S & Çelik S, Effect of particle roundness and morphology on the shear failure mechanism of granular soil under strip footing, *Acta Geotech Slov*, **15(1)** (2018) 43–53, doi: https://doi.org/10.18690/actageotechslov.15.1.43-53.2018

32 Yazıcı M F & Keskin S N, A Review on soil reinforcement technology by using natural and synthetic fibers, J Sci Technol, **14(2)** (2021) 631–663, DOI: 10.18185/erzifbed.874339

33 White D, Take W A & Bolton M D, Measuring soil deformation in geotechnical models using digital images and PIV analysis, *Proc 10th Int Conf Comput Methods ve Adv Geomechan* (Tucso: Arizona) Jan 2001, 997–1002.

34 White D J, Take W A & Bolton M D, Soil deformation measurements using particle image velocimetry (PIV) and photogrammetry, *Geotechnique*, **53** (2003) 619– 631.

35 Terzaghi K, *Theoretical Soil Mechanics* (John Wiley & Sons, Inc) 1943, DOI:10.1002/9780470172766

36 Jahanger Z K, Antony S J, Martin E & Richter L, Interaction of a rigid beam resting on a strong granular layer overlying weak granular soil: Multi-methodological investigations, *J Terramechanics*, **79** (2018) 23–32, https://doi.org/10.1016 / j.jterra.2018.05.002

37 Azzam W R & Nasr A M, Bearing capacity of shell strip footing on reinforced sand, *J Adv Res*, **6** (2015) 727–737, https://doi.org/10.1016/j.jare.2014.04.003